STET

REGULAR ARTICLE

OPEN ACCESS

Application of 3D liDAR in transmission line modeling

Zhihui Chen[*] and Shixi Fu

Power Grid EHV Transmission Company, CSG, Guangzhou 510620, PR China

Abstract. Aiming at the problem that the traditional measurement method cannot accurately obtain the line and equipment-related parameters and the line channel-related environmental parameters in the transmission line 3D modeling. In this paper, 3d liDAR technology is used to collect basic information and scan the 3d space of the power transmission line, and then the 3d model of the power transmission line is built. Conduct a three-dimensional modeling analysis using a transmission line in a certain area of Guangxi as a sample. The results show that the proposed method can accurately obtain the parameters of transmission lines and the terrain and topography of each tower, fully demonstrating the feasibility and reliability of 3D LiDAR in transmission line modeling.

1 Introduction

Transmission lines are an important channel for the transmission of electricity and a fundamental part of power system construction [1]. In order to ensure the stable operation of the power system, grid workers need to conduct regular safety inspections and patrols on transmission lines, reduce the occurrence of faults, and ensure the stable operation of transmission lines. However, the diversity and complexity of transmission lines pose challenges for identification, especially for vertically stacked lines that are difficult to accurately detect. In addition, different types of transmission lines (such as split conductors and lightning rods) have differences in functionality. Therefore, it is necessary to continuously explore and improve new technological methods to improve the accuracy and reliability of identification, modeling, and reconstruction of transmission lines.

Reference [2] conducted a study on obstacle detection on intelligent vehicle roads using laser-ranging radar and machine vision vehicle-mounted cameras. By calibrating the radar and camera, using the Retinex algorithm to enhance low light images, and combining D-S evidence theory to fuse sensor data, accurate recognition of pedestrian and vehicle information was achieved, effectively improving the efficiency and accuracy of obstacle detection. Inaccurate data fusion may lead to deviations in the spatial position and structural information of the transmission line model, affecting the accuracy and reliability of the model. Reference [3] designed an information acquisition system

based on airborne LiDAR technology for the collection and processing of traffic anomaly data. The abnormal data was identified and corrected through threshold theory and traffic flow theory, and the missing data was corrected using the Etkin interpolation algorithm, effectively solving the problem of collecting and correcting traffic anomaly data. The original data may contain noise and outliers, which need to be processed through appropriate filtering and denoising methods, otherwise, it may affect subsequent data analysis and anomaly detection. Reference [4] proposes a waveform decomposition method based on an improved differential evolution algorithm for processing full-waveform airborne LiDAR data. Through a generalized Gaussian function model and optimization algorithm, the accuracy and point accuracy of waveform decomposition are improved, thereby more effectively extracting information such as target elevation details and backscatter coefficients. Although the generalized Gaussian function model is commonly used in waveform decomposition, in certain specific cases, it may not accurately describe complex echo waveforms, thereby affecting the decomposition effect. Reference [5] analyzed the performance of laser ranging systems based on SNSPD and SPAD detectors through experiments and simulations and found that SNSPD performs better in detecting weak signal echo photons. However, when the background brightness of the skylight is too high, it will affect its signal-to-noise ratio, thereby affecting stable detection. When selecting SNSPD and SPAD detectors, if their performance characteristics and applicable scenarios are not fully understood, it may lead to unsatisfactory detection results in practical applications.

* Corresponding author: czhcsg@163.com

Lidar has advantages such as high precision, high speed, and small size. Combined with IMU inertial measurement elements and drone technology, it can quickly scan and model transmission lines and their surrounding environment [6–8]. Drones equipped with measurement equipment such as LiDAR can not only accurately obtain parameter information of transmission lines but also detect their status in real-time [9–12]. Therefore, a three-dimensional modeling method for transmission lines based on three-dimensional LiDAR is proposed in the article, which utilizes the laser ranging principle and aerial photogrammetry principle of three-dimensional LiDAR to obtain basic information data of transmission lines, restores the real-time status and parameter level of transmission lines to the greatest extent, and divides the power lines and conducts three-dimensional modeling of transmission lines, significantly improving the work efficiency of power workers and helping to timely discover potential safety hazards of transmission lines. The specific organizational structure is as follows:

Step 1: Use a drone equipped with a 3D LiDAR to collect basic information about power transmission lines and process the information data;

Step 2: Perform connectivity analysis based on TIN to identify the two-dimensional spatial range of the transmission line;

Step 3: Obtain the corresponding point cloud data of the transmission line based on the spatial range and point cloud data of the transmission line;

Step 4: Adopt an adaptive method for spatial interval division and cluster point clouds for each transmission line level;

Step 5: Use the LOAM algorithm to obtain matrix composition point cloud data and convert it according to geographic coordinates, ultimately achieving a three-dimensional reconstruction of each power line.

2 Workflow for 3D lidar in UAV power transmission line modeling

The 3D lidar on UAVs is mainly responsible for the following tasks in power transmission line modeling: obtaining basic information data, data processing, and optimization design.

1. Collection of basic information data: Firstly, the UAV equipped with 3D lidar is used, and the automatic patrol route is set using the global positioning system [13–16]. The collection process is shown in Figure 1.

The use of drones for power transmission line inspection is currently a commonly used inspection method. The control methods of drones are divided into autonomous flight and control flight [17]. Autonomous flight can be achieved by adjusting the control mode after controlling the drone to take off. Obtain point cloud data and real-time transmission line 3D data by lifting the preset flight route.

3D LiDAR achieves distance measurement of target objects by sending laser beams and measuring their return time, thus accurately perceiving the three-dimensional structure of the surrounding environment [18, 19]. This effectively improves the safety and positioning accuracy of drones, enabling them to achieve autonomous obstacle avoidance and precise positioning in complex environments. The drone adjusts its flight path in real time using point cloud information obtained from LiDAR. When obstacles approach the avoidance threshold, the drone can automatically update the avoidance flight path to reduce the impact of obstacles on flight and radar data collection [20, 21]. By combining laser radar technology with the high-altitude perspective of drones, comprehensive information about power transmission lines and their surrounding environment can be obtained. Implement basic information data collection.

1. Basic information data mainly includes flight trajectory routes, radar scanning information, environmental coordinate tags, directional and inlaid transmission line data, etc. Evaluate the quality of raw data collected by drones, including the completeness, accuracy, and presence of noise or outliers. For low-quality data, it is necessary to eliminate or correct it. Because the data collected by drones may come from different flight missions or sensors, coordinate conversion and registration techniques are used to unify them into the same coordinate system, and image processing, machine learning, and other technologies are used to recognize the features of the integrated data. Thus obtaining the basic information framework for three-dimensional modeling of transmission lines [22, 23].

2. Line optimization design: By analyzing and screening transmission line data, the UAV inspection route can be adjusted to improve the accuracy of the three-dimensional modeling of transmission lines.

3 Transmission line three-dimensional modeling

The 3D LiDAR module is shown in Figure 2.

3D LiDAR can obtain high-precision 3D point cloud data of transmission lines and their surrounding environment by emitting laser beams and measuring their return time. These data not only contain distance information but also angle and intensity information, providing a rich data source for subsequent modeling.

3.1 Identification of two-dimensional spatial range for transmission lines

Directly processing and filtering a large amount of transmission line coordinate data may be complex and inefficient. By identifying the two-dimensional spatial range of transmission lines, it is possible to quickly screen out areas that require detailed modeling, reducing the complexity and workload of data processing. During the model construction process, if errors are found in certain areas or need to be corrected, they can be quickly located to the corresponding positions through two-dimensional spatial range identification for correction and optimization.
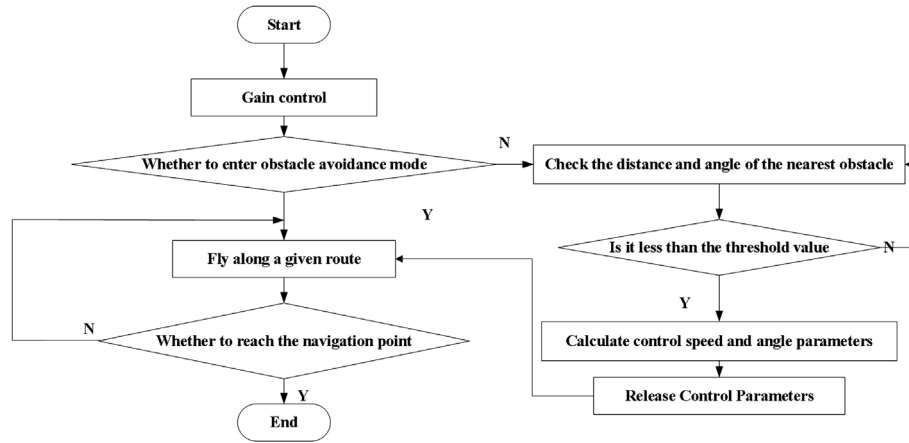
Figure 1. UAV flight process.

The two-dimensional spatial range identification of transmission lines needs to be precise to specific positions and shapes for subsequent 3D modeling and operation management. An Irregular Triangle Network (TIN) can accurately describe the coverage range of transmission lines on the ground, including key elements such as towers, conductors, terrain, etc. [24], providing accurate basic data for two-dimensional spatial range identification.

Using spatial clustering method to calculate the similarity between the coordinates of transmission lines and categorize similar data points into one category. Identify the main paths and key points of the transmission line, namely the transmission line and tower points. Significantly reduce the number of data points involved in TIN construction, thereby improving computational efficiency and data quality. The recognition result is shown in Figure 3.

On this basis, the two-dimensional spatial range of the transmission line is identified through connected component analysis based on TIN, and the results are shown in Figure 4.

3.2 Determination of 2D spatial range and transmission line point cloud for each gear

The two-dimensional spatial range identification mainly focuses on the horizontal layout, but it is usually only divided into one layer in the vertical direction, so it cannot fully reflect the true layout of the line in three-dimensional space. By determining the two-dimensional spatial range of each level, different areas of the transmission line can be accurately divided, providing accurate spatial references for subsequent 3D modeling. At the same time, as the basic data for 3D modeling, the point cloud of transmission lines can record detailed 3D coordinate information of transmission lines and their surrounding environment, thereby improving the accuracy and precision of modeling. Therefore, the basic information obtained from the three-dimensional LiDAR carried by the drone is analyzed to obtain the spatial range and point cloud data of the transmission line as shown in Figure 5.

The 3D model of the transmission line is composed of a horizontal projection model and a vertical projection model.
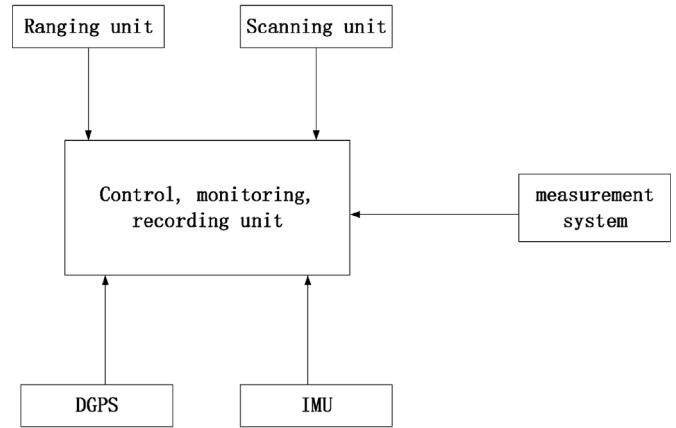

Figure 2. System composition.

The horizontal projection model is based on the X/Y plane, and the vertical projection model can be obtained from the x/z plane or y/z plane [25]. The horizontal projection model locates two towers separated by transmission lines to obtain an external rectangle, the length of which corresponds to the routing and length of the transmission line [26]. The range of values in the X and Y axes is x_{range} and y_{range}. The formulas for both are

$$x_{\mathrm{range}} = x_{\max} - x_{\min} \tag{1}$$

$$y_{\mathrm{range}} = y_{\max} - y_{\min} \tag{2}$$

In the formula, $x_{\max}$ and $x_{\min}$ are respectively the maximum and minimum values of the x coordinate of the transmission line, while $y_{\max}$ and $y_{\min}$ are respectively the maximum and minimum values of the y coordinate of the point of the transmission line.

The formula for the three-dimensional model of the transmission line is as follows
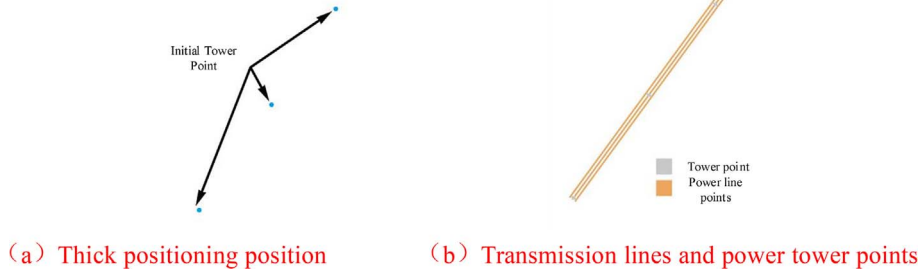
The linear model formula is

$$y = kx + b \tag{3}$$

<center>（a）Thick positioning position   （b）Transmission lines and power tower points</center>

Figure 3. Recognition results based on spatial clustering.

<center>(1) Point cloud   (2) Enlarged view of the tower</center>

<center>(3) Minimum   (4) Two-dimensional   (5) Modeling overlay
bounding rectangle   spatial range   result</center>
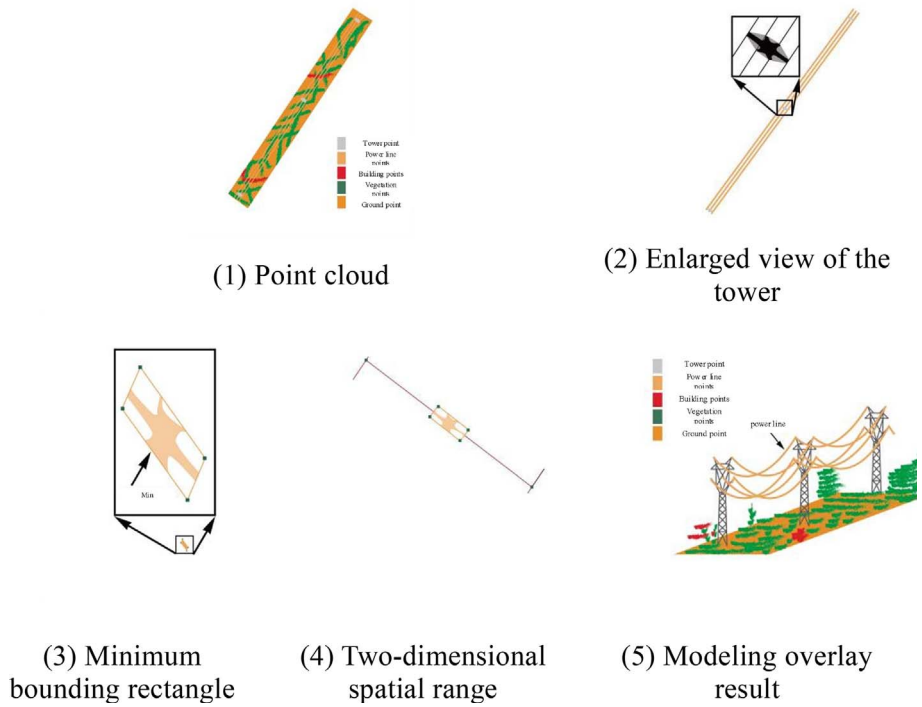
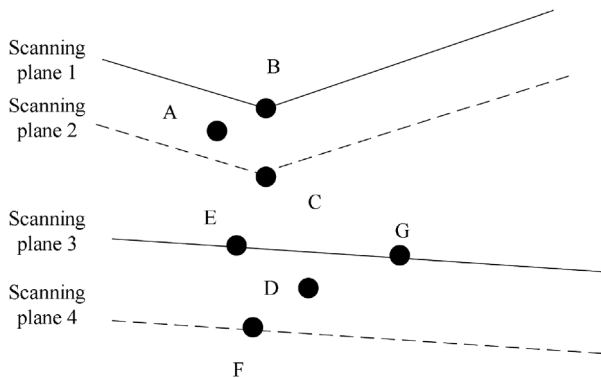**Figure 4.** Results of two-dimensional spatial range identification for transmission lines.

Figure 5. Transmission line scan data matching.

The parabolic model formula is

$$z = a_0 x^2 + a_1 x + a_2 \left(x_{range} \geq y_{range} \right) \tag{4}$$

Or

$$z = a_0' x^2 + a_1' y + a_2' \left(x_{range} < y_{range} \right) \tag{5}$$

In the equation, k and b represent the slope coefficients and constant coefficients in the linear function model respectively, and a_0, a_3 is the coefficients in the quadratic arc function.

According to the order of clockwise, the two-dimensional space of the transmission line is constructed by minimum matrix. Different colors are used for matrix coloring to obtain point cloud data of transmission lines.

The characteristic point smoothness of transmission lines is expressed as

$$c = \frac{1}{|S| \cdot \left| X_{(k,i)}^L \right|} \left\| \sum_{j \in S, j \neq i} \left(X_{(k,i)}^L - X_{(k,j)}^L \right) \right\| \qquad (6)$$

The smoothness of feature points can reflect the curvature, shape, and continuity of transmission lines at specific positions. The distance between the feature edge point and the corresponding line segment can be expressed as follows

$$de = \frac{\left| \left(X_{(k,A)}^L - X_{(k-1,B)}^L \right) \times \left(X_{(k-1,B)}^L - X_{(k-1,C)}^L \right) \right|}{\left| \left(X_{(k-1,B)}^L - X_{(k-1,C)}^L \right) \right|} \qquad (7)$$

The formula of the distance from the point of the characteristic plane to the corresponding plane is like the expression (3)

$$de = \frac{\left| \left(X_{(k,D)}^L - X_{(k-1,E)}^L \right) \times \right.}{\left| \left(X_{(k-1,E)}^L - X_{(k-1,F)}^L \right) \times \right.} \rightarrow$$
$$\leftarrow \frac{\left(X_{(k-1,E)}^L - X_{(k-1,F)}^L \right) \times \left(X_{(k-1,E)}^L - X_{(k-1,G)}^L \right) \right|}{\left. X_{(k-1,E)}^L - X_{(k-1,G)}^L \right|} \qquad (8)$$

The motion estimation point cloud transformation expression is

$$\tilde{X}_{(k,i)}^L = R_{(k,i)}^L X_{(k,i)}^L + \tau_{(k,i)}^L \qquad (9)$$

3.3 Point cloud clustering for each transmission line

Due to the discontinuity of terrain, the possibility of "fractures" in the power lines themselves, or the large difference in maximum elevation between adjacent power line grids, these factors may lead to "fractures" in the power line point cloud, affecting the integrity of the 3D model. Adopting an adaptive approach for spatial interval division, along the direction of the power line, the transmission line points in the entire area are divided into several segments. It can be found that the various power lines within the local range of each segment are basically parallel, which helps identify and repair the "broken" part of the power line point cloud, and improves the integrity and accuracy of the 3D model. The clustering process is as follows:

1. Linear fitting of horizontal coordinates of transmission lines by using the least squares method [27].
2. Obtain the arrangement order of the points according to the projection of the transmission line on the XOY plane, and calculate the position difference of the horizontal direction between the endpoints (unit: m), N represents the total number of segments, and the calculation formula is

$$N = da(3) \qquad (10)$$

   In the formula: a the empirical length threshold.
3. Assigning transmission line points of different grades to corresponding time periods according to the characteristics of scale factors.

4. The whole three-dimensional reconstruction shall be applied to the transmission line points of each section [28, 29].
5. Centralize the projection of all transmission line points in this section as shown in Figure 6.

The LOAM algorithm can reduce the time required for point cloud registration and improve real-time performance. When performing pose interpolation calculations, this high real-time performance ensures the rapid processing and updating of point cloud data, thereby improving the accuracy of point cloud clustering. The interpolation formula of pose using the LOAM algorithm is

$$T_{(k+1,i)}^L = \frac{t_i - t_{k+1}}{t - t_{k+1}} T_{(k+1)}^L \qquad (11)$$

The corresponding relationship of transmission line data points collected by 3D laser radar is as follows

$$X_{(k+1,i)}^L = R\tilde{X}_{(k+1)}^L + T_{(k+1,i)}^L(1:3) \qquad (12)$$

Where the expansion of the R matrix is

$$R = e^{\hat{\omega}\theta} = I + \hat{\omega}\sin\theta + \hat{\omega}^2(1 - \cos\theta) \qquad (13)$$

The distance from point to surface and from point to line can be obtained by derivation of the rotation matrix, and the error function can be used for optimization.

$$f\left(T_{k=1}^L \right) = d \qquad (14)$$

f contains a number of lines, where each line represents a feature point. Point cloud clustering usually involves optimization problems, such as minimizing the distance between points and cluster centers. The Jacobian matrix is a key tool for solving such optimization problems, providing information on the partial derivatives of the objective function relative to the optimization variables. Therefore, the Jacobian matrix will be solved later. The point cloud clustering process typically involves nonlinear optimization problems. The Jacobian matrix provides information on the partial derivatives of the objective function with respect to the optimization variables. LM methods update the search direction based on the Jacobian matrix information of the current point and perform a one-step search along that direction. Through multiple iterations, the LM method can gradually approach the optimal solution, thereby achieving optimized clustering of point cloud data. The process of implementing optimization using the LM method is as follows:

$$T_{k+1}^L \leftarrow T_{k+1}^L \left(J^T J + \lambda idag(J^T J) \right)^{-1} J^T d \qquad (15)$$

In the process of point cloud clustering for transmission lines, it is necessary to unify point cloud data from different sources and poses into the same coordinate system for accurate clustering analysis. The ICP algorithm is mainly used in point cloud data processing to solve the registration problem of two or more sets of point clouds from different perspectives and reference coordinates. Therefore, the objective function S is minimized by the corresponding points of the ICP algorithm, and the formula is
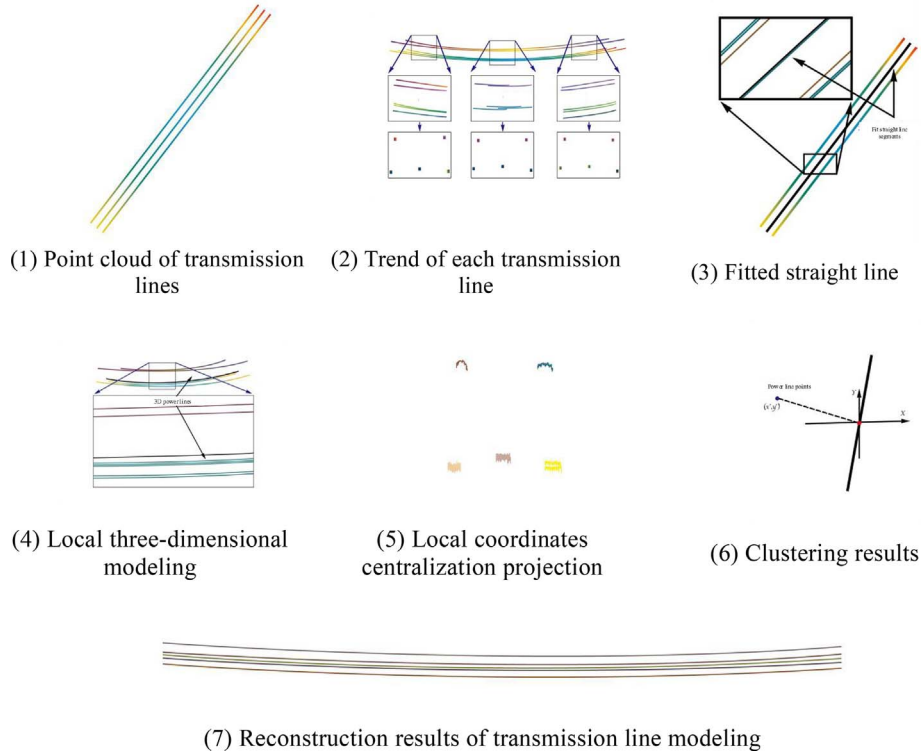
(1) Point cloud of transmission lines

(2) Trend of each transmission line

(3) Fitted straight line

(4) Local three-dimensional modeling

(5) Local coordinates centralization projection

(6) Clustering results

(7) Reconstruction results of transmission line modeling

Figure 6. Example of 3D modeling of single-speed transmission line.

$$S^2 = \min \sum\nolimits_{t=1}^{N} \left\| Q_i - (RP_i + t) \right\|^2 \qquad (16)$$

M is the number of updates, SI is the point in the reference point cloud, P_i is the corresponding point in the transmission line point cloud, R and t are the point cloud rotation matrix of the transmission line matrix. By applying the point cloud rotation matrix, point cloud data can be transformed from the original coordinate system to a coordinate system that is more conducive to clustering, thereby optimizing clustering performance.

In summary, point cloud clustering can accurately identify and segment point cloud data of a single power line, avoiding confusion and interference between different power lines. This ensures the accuracy and reliability of subsequent 3D modeling.

3.4 3D reconstruction of each power line

Although clustering can divide point cloud data into different categories, the clustering results may not be entirely accurate, resulting in misclassified or unclassified point cloud data. This may lead to errors or omissions in the subsequent 3D reconstruction process. The LOAM algorithm can accurately calculate the pose of LiDAR and convert point cloud data into an unified geographic coordinate system based on pose information. This transformation can eliminate errors caused by differences between different coordinate systems, thereby improving the accuracy of 3D reconstruction [30]. Therefore, the point cloud data obtained by the LOAM algorithm is transformed according

to the geographic coordinates, and the 3D reconstruction of each power line is realized. After the reconstruction of each power line, the distance between the reconstructed 3D model and each transmission line point can be kept according to the criterion of three times the standard deviation. The results of 3D reconstruction of a model with 10 power lines in multiple stalls shown in Figure 4 (1) are shown in Figure 4 (5), where the reconstructed model is seen to be highly consistent with the original point cloud; the results of 3D reconstruction of a model with 5 power lines in a single stall shown in Figure 6 (1) are shown in Figure 6 (7), where the reconstructed model is seen to be completely consistent with the original point cloud.

The process of three-dimensional modeling of transmission lines is shown in Figure 7.

4 Experimental analysis

This paper is based on the Visual Studio 2009C++ integrated development environment to achieve three-dimensional modeling of transmission lines. The parameters of 3D modeling include prior parameters (number of transmission lines M, diameter D) and empirical parameters. In the research, the transmission line under 500 kV in a certain place in Guangxi is applied. There are many large trees in this area, so there are some safety risks in collecting transmission line parameters and inspecting transmission line safety. The total length of the test data line is 890 m, each gear contains 5 power lines, the height difference
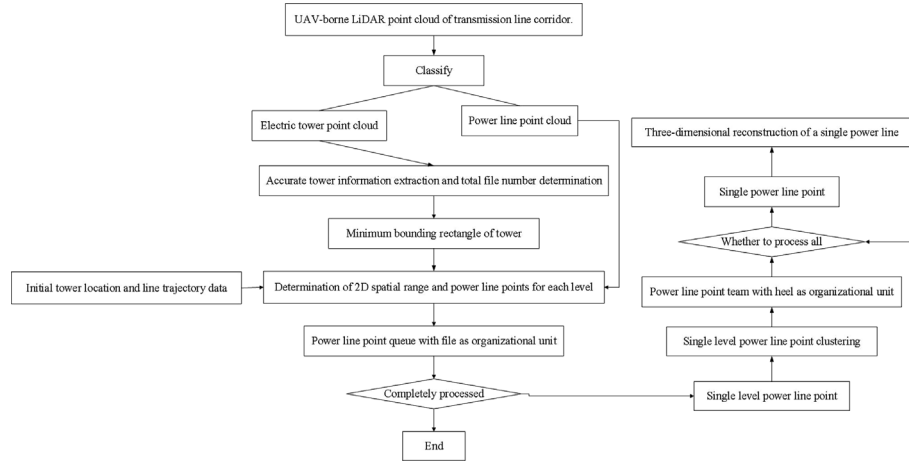
Figure 7. Modeling process.

Table 1. System hardware.

Hardware name	Hardware models	
Drone	Mavic Air2	
Three-dimensional lidar	Velodyne VLP-16	
Processor models	NVIDIA Tegra	
Positioning module	BX 430	
Resolution of aerial camera	50 million pixels	
Flight altitude	200 m	Ensure sufficient coverage and image resolution
The length of the straight section of the route	≤1 km	Ensure complete coverage of transmission line corridors
Lateral overlap rate	50%	To provide sufficient image overlap
Flight speed	8 m/s	Ensure clarity and stability of images

between adjacent towers is 15 m, and the power line width is 100 m. The system hardware is shown in Table 1.

The parameter settings of the algorithm during the experiment are shown in Table 2.

Due to the limitation of flight requirements, UAV in Dajiang is used to carry out 3D lidar. There were three experimental flights: the first to assess the transmission line environment and flight quality, and the second to improve the quality of data acquisition by adjusting the flight altitude and speed. This flight was set at an altitude of 220 m with a speed of 70 km/h; the third flight (i.e. return) was at a height of 50 m at a speed of not more than 40 km/h, and the data obtained from 3D laser radar scanning is shown in Figure 8.

The collected data are sampled by the filter, matched, and registered, and the observation point cloud of the radar coordinate system and transmission line is obtained. The smoothness of the feature plane can be calculated as 0.19 after the point cloud sequence is input. By inputting the set of edge points into the formula (3), the maximum distance between the feature plane points and the corresponding plane is 74.6755 m, the minimum value is 0.0655, the average value is 15.4722 m, and the error is 2.2%.

Three-dimensional laser point cloud images of transmission lines and objects nearby can be generated by processing and restoring the acquired data, as shown in Figure 9.
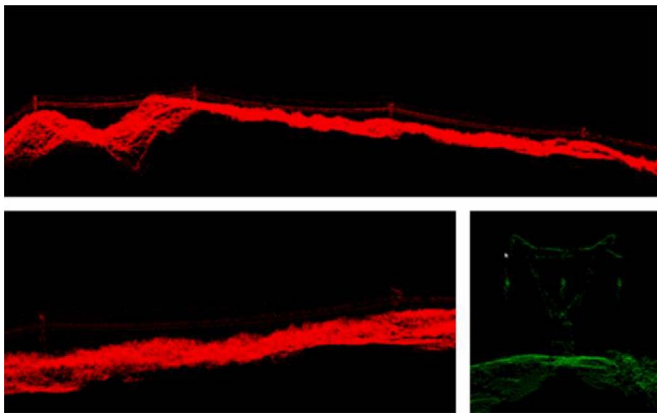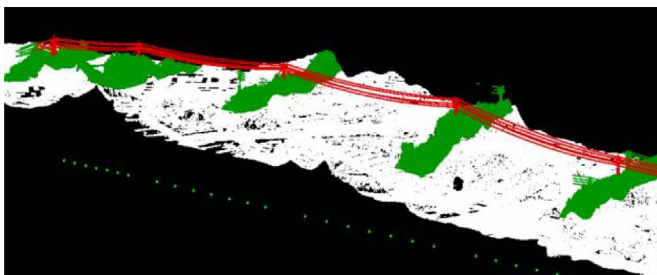
In this paper, the same transmission line in the Three Gorges region is scanned and analyzed. The large airborne 3D laser scanning equipment is scanned by a helicopter, and the distance between the points and lines is used as a precision evaluation index. The final parameters collected are shown in Figure 10 to meet the expected requirements of the project.

The 1#-5# tower of the dark mark was compared with the light mark of the large airborne 3-D laser scanning equipment, and the scanning line tower data were found to be completely consistent. Therefore, on the basis of proper combination, strict implementation of technical plans, and evasion of potential risks, the flight platform can be combined with field data collection equipment at will. The accurate transmission line parameters and the topography of the towers can be obtained by using light and small-size 3D laser radar. The parameters are also in the range of technical index.

In order to more intuitively verify the effectiveness of the projection model in modeling transmission lines, the
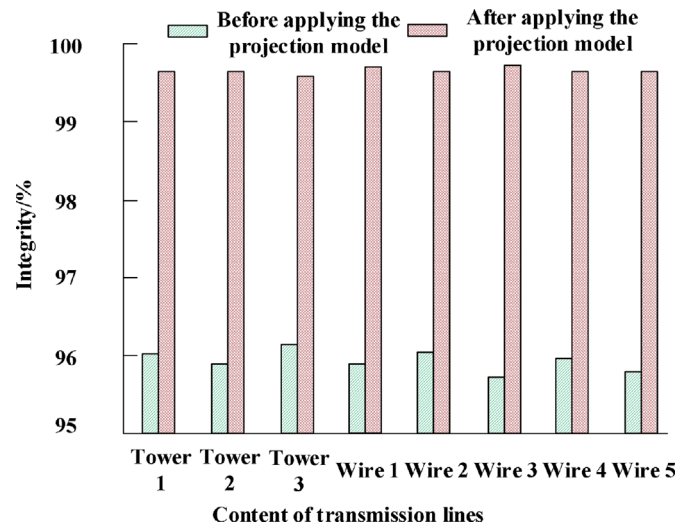
Table 2. Algorithm parameter settings.

Parameter name	Parameter values
Neighborhood radius	2 m
Minimum sample size	5
LOAM algorithm pose interpolation interval	0.1 s
The number of iterations for solving the Jacobian matrix	50
LM optimization convergence threshold	1e−6
ICP algorithm corresponding point distance threshold	0.05 m
TIN construction with maximum triangle side length	5 m
TIN construction minimum angle	30°
Location accuracy of transmission lines	±0.5 m
Shape accuracy (resolution) of transmission lines	1 m
3D model accuracy (wire diameter error)	≤1 cm
3D model accuracy (tower height error)	≤0.5 m

Figure 8. 3D data of transmission lines.

Figure 9. Transmission line laser point cloud.

Figure 10. Comparison of collection methods.

Figure 11. Integrity of transmission line models.

completeness of the transmission line model before and after the application of the projection model is compared. The results are shown in Figure 11.

According to the analysis of Figure 11, the application of the projection model can improve the integrity of the transmission line model to over 99%. Effectively ensuring the construction effect of the transmission line model.

Selecting references [2] and [3] as the comparative methods of our method, the feature recognition rate is used as the evaluation index to evaluate the system's ability to identify transmission line components (such as towers and conductors). The verification results are shown in Figure 12.

Analyzing Figure 12, it can be seen that as time increases, the feature recognition rates of the three methods
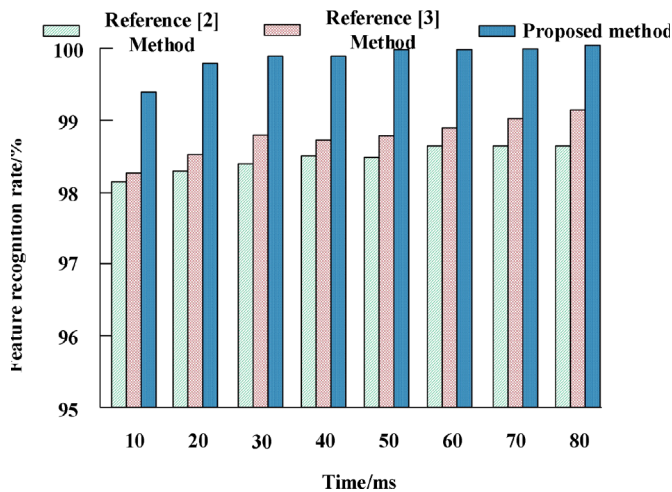
Figure 12. Result of feature recognition rate.

all show an upward trend. Among me, the feature recognition rate of the proposed method has remained above 99%. This is because the proposed method can accurately describe the complex morphology of terrain and transmission lines on the ground through TIN, including key elements such as towers and conductors. This provides accurate basic data for subsequent 3D modeling. Therefore, the proposed method can effectively identify the components of transmission lines, construct precise 3D models, and accurately reflect the actual structure and layout of transmission lines.

Three-dimensional lidar realizes automatic 3D reconstruction of power lines with high precision, strong adaptive ability, and high robustness. Different types of multi-wire 3D reconstruction can be achieved using 3D lidar, including single conductor, split conductor, lightning conductor, and so on. This method can weaken the distance difference, irregular break of point cloud, and interference of coarse error. The reconstruction result is consistent with the original point cloud.

5 Conclusions

Transmission lines are often affected by the natural environment, such as lightning, strong winds, rain and snow, and other adverse weather conditions. In this paper, the transmission line data are scanned and the 3D modeling is carried out by UAV with 3D laser radar. Data acquisition, monitoring, and precise modeling of power transmission lines and their related environments are realized by using the Dajiang UAV as a mature flight platform. By planning the UAV route in advance, the UAV automatic route tracking and route modeling information can be obtained automatically, and the terrain information can be obtained by 3D laser radar. Experiments show that the proposed method can reduce the influence on the model caused by the difference in 3D space arrangement, power line type, coarse difference, irregular break of point cloud, and line length. Through data acquisition and 3D visualization modeling of the

transmission line, the feasibility of the proposed scheme is verified, and it plays a good demonstration role and effect in practical application. However, current methods mainly focus on modeling transmission lines in static environments, but the state of transmission lines may change over time (such as tree growth, line aging, etc.). Therefore, in the future, real-time and dynamic transmission line modeling technology should be studied, which can monitor the status changes of transmission lines in real time and quickly update the three-dimensional model, providing strong support for the safe operation of the power system.

In summary, by scanning transmission line data and conducting 3D modeling for special and nighttime inspections, staff can timely detect abnormal phenomena and component deformation and damage in the event of sudden climate changes or natural disasters, and take corresponding preventive measures to reduce the occurrence rate of faults.

Conflicts of interest

The author(s) declared no potential conflicts of interest with respect to the research, authorship, and/or publication of this article.

Ethical approval

This article does not contain any studies with human participants or animals performed by any of the authors.

Data availability statement

The datasets generated during and/or analyzed during the current study are available from the corresponding author upon reasonable request.

References

1 Yu S., Yiqing X., Longxiang C. (2011) Research on optimal planning of high voltage distribution network[J], *Power Grid Technol.* **35**, 10, 70–75.
2 Hongbin Y., Huiqun C., Qunyong O. (2021) Obstacle detection based on laser ranging radar and machine vision [J], *Mod. Radar* **43**, 5, 57–62.
3 Jiangong Z. (2021) Research on airborne lidar traffic anomaly data acquisition and data processing [J], *Mod. Radar* **43**, 9, 63–68.
4 Xudong L., Yifei Y., Jingzhong X., Mingwei W. (2021) Waveform decomposition of airborne lidar based on improved differential evolution algorithm [J], *J. Infrar. Millimeter Waves* **40**, 3, 381–390.
5 Xiaoying Z., Lei J., Jiang Z., Xiachao Y., Xiaobao Z., Lin K., Peiheng W. (2018) Comparison of laser ranging system based on SNSPD and SPAD detector [J], *J. Infrar. Millimeter Waves* **37**, 3, 378–384.
6 Feng M., Gao X., Wang J., et al. (2021) Research on vehicle target shape position fusion algorithm based on stereo vision and LiDAR [J], *J. Instrum. Meters* **42**, 10, 11–13.

7 Ming L., Zishu H.E. (2021) Selection algorithm of training samples for airborne radar based on output signal-to-noise ratio [J], *J. Univ. Electron. Sci. Technol. China* **50**, 5, 6–12.

8 Jiajia G., Changyuan Z., Liping C., et al. (2021) Based on laser radar tree canopy leaf area target detection model research [J], *J. Agric. Mach.* **52**, 11, 9–14.

9 Shuai Y., Xiang Y., Jingxian X., et al. (2021) Based on the deep study of cognitive imaging laser radar (guest) [J], *J. Photon* **50**, 10, 10–13.

10 Zhou Z.G., Cao J.W., Di S.F. (2021) Overview of 3D lidar SLAM algorithms [J], *J. Instrum. Meters* **42**, 9, 15–18.

11 Xiangda L., Hongtao W., Zongze Z. (2021) Integrated transfer learning and full convolutional networks for point cloud classification of small sample airborne lidar [J], *Chin. J. Lasers* **48**, 16, 138–149.

12 Jia W., He W., Wu L., et al. (2022) Polarized laser radar polarization aberration correction of telescopic system [J], *J. Opt.* **42**, 2, 7–12.

13 Qichao W., Songhua W., Hongwei Z., Bingyi L., Kailin Z. (2021) Observation and data processing of offshore wind field by unmanned aerial vehicle Doppler lidar [J], *J. Infrar. Millimeter Waves* **40**, 4, 516–529.

14 Li J., Shao J., Wang R., et al. (2021) A closed-loop detection algorithm for lidar point cloud based on SR-context [J], *J. Opt.* **41**, 22, 11–15.

15 Xu H., Zhi L., Yaojun W., et al. (2022) Pseudo random code modulation precision spaceborne laser ranging radar [J], *Infrar. Laser Eng.* **51**, 3, 9–13.

16 Chaojie W., Renpeng Y., Xudong L., Xiangxi M., Xinyang L. (2021) Research progress of sub-nanosecond lasers for 3D imaging lidar applications[J], *Opt. Precis. Eng.* **29**, 6, 1270–1280.

17 Jinyue L., Xu T., Xiaohui J., Wenfeng X., Tiejun L. (2020) *Chin. J. Sci. Instrum.*, **41**, 7, 99–106.

18 Liang Z., Jie H., Han L., Yongpeng A., Zongquan X., Wang Y. (2021) Deep learning laser point cloud 3D target detection algorithm based on semantic segmentation[J], *China Laser* **27**, 6, 1–22.

19 Bingqing X., Yan H., Wenjing X., Jun Z., Dongsong S. (2021) *Infrar. Laser Eng.* **50**, 9, 192–200.

20 Zhangfei W., Chunyang L., Xin S., Fang Y., Xiqiang M., Lihai C. (2020) 3d point cloud target segmentation and collision detection based on depth projection [J], *Opt. Precis. Eng.* **28**, 7, 1600–1608.

21 Guoyan X., Huan N., Chenyang G., Hongjie S. (2020) Research on target recognition and tracking based on 3d laser point cloud [J], *Autom. Eng.* **42**, 1, 38–46.

22 Yanwei H., Jianjun W., Yuanyuan F., Yunpeng L., Chongyue B., Qiyun Z. (2020) Three-dimensional modeling and volume calculation of space objects based on lidar [J], *Chin. J. Lasers* **47**, 5, 496–505.

23 Jinyue L., Xu T., Xiaohui J., Dong Y., Tiejun L. (2019) *Chin. J. Sci. Instrum.* **40**, 11, 64–72.

24 Jiangong Z. (2021) Research on airborne lidar traffic anomaly data acquisition and data processing [J], *Mod. Radar* **43**, 9, 63–68.

25 Mianrong Y., Liping N. (2020) Research on geospatial element recognition algorithm based on lidar [J], *Mod. Radar* **42**, 12, 56–61.

26 Centeno J.A., Silva C.R. (2022) Evaluation of LiDAR point clouds density in the interpolation of digital terrain models for power line planning in Northeast Brazil, *Anuário do Instituto de Geociências* **45**, 1–15.

27 Bhutada S., Shah J.P., Dhiman G., Chetwani S., Subramanian S.S., Subba Rao P.V. (2020) 3D electric field modelling of UHV class AC composite transmission line insulators, in: *2020 21st National Power Systems Conference (NPSC)*, pp. 1–6.

28 Santana J., Ortega S., Santana J.M., Trujillo A., Suárez J.P. (2018) Noise reduction automation of LiDAR point clouds for modeling and representation of high voltage lines in a 3D virtual globe, in: *Spanish Computer Graphics Conference*.

29 Tebaldini S., d'Alessandro M.M., Ulander L.M.H., Bennet P., Gustavsson A., Coccia A., Macedo K., Disney M.I., Wilkes P., Spors H.-J., Schumacher N., Hanuš J., Novotný J., Brede B., Bartholomeus H.M., Lau A., van der Zee J., Herold M., Schuettemeyer D., Scipal K. (2023) TomoSense: a unique 3D dataset over temperate forest combining multi-frequency mono- and bi-static tomographic SAR with terrestrial, UAV and airborne lidar, and in-situ forest census, *Remote Sens. Environ.* **290**, 113532.

30 Kočí J. *Self-localization of an unmanned aerial vehicle in the transmission tower inspection task*, 2022.